Journal of The
Electrochemical Society

Dusty-Gas Model Conservation Law and Approximate Analytical Solutions for $H_2 - H_2O$ Transport in the SOFC Anode Support Layer

To cite this article: Andrei Kulikovsky 2025 *J. Electrochem. Soc.* **172** 014510

Journal of The Electrochemical Society, 2025 **172** 014510

Dusty-Gas Model Conservation Law and Approximate Analytical Solutions for H_2-H_2O Transport in the SOFC Anode Support Layer

Andrei Kulikovsky[*,z]

Forschungszentrum Jülich GmbH, Theory and Computation of Energy Materials, Institute of Energy and Climate Research, D–52425 Jülich, Germany

A complete Dusty-Gas Model for the H_2–H_2O mixture in the anode transport layer of the anode-supported SOFC is considered. An exact conservation law relating the total pressure and the hydrogen molar fraction at any point in the anode to their values in the anode channel is derived. Using this conservation law, approximate analytical solutions for the hydrogen molar fraction and total pressure in the anode transport layer are obtained. Possible appliucations of the solutions are discussed. A condition for neglecting the pressure gradient is derived.

 [DOI: 10.1149/1945-7111/adab2a]

Manuscript submitted October 1, 2024; revised manuscript received January 4, 2025. Published January 29, 2025.

List of Symbols

~	Marks dimensionless variables
B_0	Hydraulic permeability, m^2, Eq. 31
c	Hydrogen molar concentration, mol m^{-3}
c_a	Hydrogen molar concentration at the active layer, mol m^{-3}
D_m	Effective binary molecular diffusion coefficient in H_2–H_2O mixture, $m^2\ s^{-1}$
$D_{K,h}$	Effective Knudsen diffusion coefficient of hydrogen, $m^2\ s^{-1}$
$D_{K,w}$	Effective Knudsen diffusion coefficient of water, $m^2\ s^{-1}$
d	Mean pore diameter, m
F	Faraday constant, C mol^{-1}
J	Cell current density, A m^{-2}
K	$\equiv D_{K,h}/D_m$
L	Anode support layer thickness, m
M_i	Molecular weight of the ith component, kg mol^{-1}
N_i	Molar flux of the ith component, mol $m^{-2}\ s^{-1}$
p	Pressure, Pa
p_*	Characteristic pressure, Pa, Eq.9
Q	$\equiv\sqrt{M_w/M_h} = 3$
R	Gas constant, J K^{-1} mol^{-1}
T	Cell temperature, K
W	$\equiv\partial\tilde{p}/\partial\tilde{x}\vert_{\tilde{x}=0}$, Eq.18
x	Coordinate through the anode support layer, m
y	Molar fraction of hydrogen
y_i	Molar fraction of the ith component
Subscripts:	
*	Characteristic value
a	ASL/active layer interface
c	Channel/ASL interface
h	Hydrogen
K	Knudsen diffusion
m	Molecular diffusion
t	Total molar concentration
w	Water
Greek:	
η_{tra}	Anode transport overpotential
λ	Porosity/tortuosity ratio
μ	Dynamic viscosity, Pa s

Anode–supported Solid Oxide Fuel Cells (SOFCs) employ a thick, on the order of 1 mm, porous anode support layer (ASL). The role of the ASL is threefold: (i) it provides mechanical stability to the SOFC sandwich, (ii) it serves as a transport layer for gases, and (iii) it transports electrons from the active layer to the external circuit.

Mass transport through porous media is a classic problem in chemical engineering.[1] The huge surface area of pores dramatically increases the rate of surface–activated chemical or electrochemical reactions. In some devices, part of the porous domain is used for diffusive transport of gaseous or liquid components to/from the reaction zone. An important example is the anode–supported SOFC, where the porous ASL provides transport of hydrogen to and water vapor from the thin reaction zone located near the electrolyte.[2]

Schematic of the SOFC anode is shown in Fig. 1. Hydrogen is supplied through the channel in the interconnect to the porous ASL, and finally to the active layer, where the electrochemical conversion of H_2 runs

$$H_2 + O^{2-} \rightarrow H_2O + 2e^- \qquad [1]$$

The oxygen ions O^{2-} enter the active layer from the cathode side through the electrolyte. The product water is removed through the ASL to the channel / interconnect. The ASL thus supports two opposite fluxes of hydrogen and water vapor.

It has been agreed that the most general description of multi-component gas transport in porous media is provided by the Dusty–Gas Model (DGM).[1,3,4] The DGM equation for the molar fraction y_k of the kth component of a gaseous mixture is (Zhu and Kee[3]):

$$\sum_{i\neq k}\frac{y_iN_k - y_kN_i}{D_{ik}} + \frac{N_k}{D_{K,k}} = -\frac{1}{RT}\left(\frac{\partial(y_kp)}{\partial x} + \frac{y_k}{D_{K,k}}\frac{pB_0}{\mu}\frac{\partial p}{\partial x}\right) \qquad [2]$$

or, collecting the terms with the pressure gradient,

$$\sum_{i\neq k}\frac{y_iN_k - y_kN_i}{D_{ik}} + \frac{N_k}{D_{K,k}} = -\frac{p}{RT}\frac{\partial y_k}{\partial x} - \frac{1}{RT}\left(y_k + \frac{y_k}{D_{K,k}}\frac{pB_0}{\mu}\right)\frac{\partial p}{\partial x} \qquad [3]$$

Here N_k is the molar flux of the kth component, p the pressure, $D_{i,k}$ the effective binary molecular diffusion coefficient, $D_{K,k}$ the effective Knudsen diffusion coefficient, B_0 the hydraulic

*Electrochemical Society Member.
[z]E-mail: A.Kulikovsky@fz-juelich.de

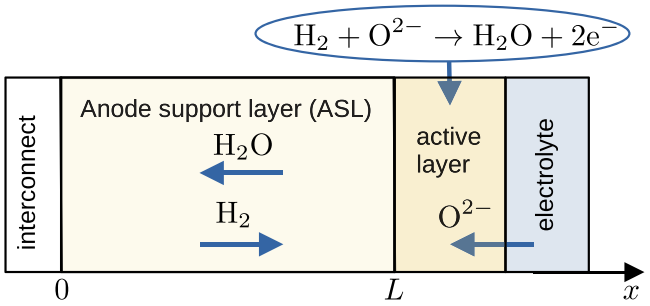

Figure 1. Schematic of anode–supported SOFC anode. The sketch is strongly not to scale: the active layer thickness is two orders of magnitude smaller than the ASL thickness.

permeability of the porous media, μ the mixture viscosity. The DGM takes into account the inter–diffusion Stefan–Maxwell fluxes (the first term on the left side), the Knudsen diffusion in smaller pores (the second term on the left side), and the flux due to the pressure gradient (the last term in Eq. 3).

The pressure gradient term introduces considerable complexity to the analysis and in many works this term has been neglected.[5–10] This simplifies the DGM, Eq. 3, to the Stefan–Maxwell–Knudsen Model (SMKM):

$$\sum_{i\neq k}\frac{y_i N_k - y_k N_i}{D_{ik}} + \frac{N_k}{D_{K,k}} = -\frac{p}{RT}\frac{\partial y_k}{\partial x} \qquad [4]$$

An exact consequence of SMKM is the Graham's law[11]

$$\sum_k N_k\sqrt{M_k} = 0 \qquad [5]$$

Eq. 5 is obtained by summing Eq. 4 over k, taking into account that the Stefan–Maxwell terms cancel, the sum $\Sigma_k y_k = 1$, and $D_{K,k}\sim 1/\sqrt{M_k}$, where M_k is the molecular weight of the kth component. However, in the SOFC anode, the water and hydrogen fluxes are related by the stoichiometric requirement $N_w = -N_h$, which follows from Eq. 1. The relation $N_w = -N_h$ is provided by the pressure gradient, which is missing in SMKM.

Several works have demonstrated the importance of the pressure gradient term[12–14] (note a typo in Eq. (35a) of Ref. 13). Fu et al.[4] have shown that the inequality of the Knudsen diffusion coefficients of hydrogen and water creates a pressure gradient in the porous media. Indeed, in a two–component system, if $M_1 = M_2$, the Graham's law, Eq. 5, reduces to the required SOFC anode stoichiometry relation $N_1 + N_2 = 0$. Thus, if the molecular weights of water M_w and hydrogen M_h were equal, the SMKM would be equivalent to the DGM. In fact, however, $\sqrt{M_w/M_h} = 3$, which makes the things more complicated. Bertei and Nicolella[14] discussed this and several other inconsistencies in models for porous electrodes.

In this work, a complete two–component DGM for the H_2–H_2O transport in the SOFC ASL is considered. An exact conservation law is derived that relates the total pressure and hydrogen molar fraction at any point in the anode to their values in the channel. The conservation law is used to construct approximate analytical solutions to the DGM equations. Comparison with numerical results shows good accuracy of the analytical formulae. A condition for neglecting the pressure gradient is derived.

Model

Two–component DGM equations.—The equation for the hydrogen molar fraction $y \equiv y_h$ in the two–component mixture of H_2–H_2O is obtained from Eq. 2 taking into account that $y_w = 1 - y$ and $N_w = -N_h$:

$$\frac{\partial(yp)}{\partial x} + \frac{ypB_0}{D_{K,h}\,\mu}\frac{\partial p}{\partial x} = -\frac{RT}{D_{K,h}}(1+K)N_h \qquad [6]$$

where the subscripts w and h denote water and hydrogen, respectively. The equation for the total pressure is obtained by summing Eq. 3. It is easy to verify that for the H_2–H_2O mixture $\Sigma_k y_k/D_{K,k} = (Q + y(1-Q))/D_{K,h}$. Taking into account that the Stefan–Maxwell terms cancel and $\Sigma_k y_k = 1$we get

$$\left(1 + (Q + y(1-Q))\frac{pB_0}{D_{K,h}\,\mu}\right)\frac{\partial p}{\partial x} = -\frac{RT}{D_{K,h}}(1-Q)N_h \qquad [7]$$

Here,

$$K = \frac{D_{K,h}}{D_m}, \quad Q = \frac{D_{K,h}}{D_{K,w}} = \sqrt{\frac{M_w}{M_h}} = 3. \qquad [8]$$

The factor $pB_0/(D_{K,h}\,\mu)$ in Eqs. 6, 7 suggests a suitable characteristic scale for pressure. Introducing dimensionless variables

$$\tilde{x} = \frac{x}{L}, \quad \tilde{p} = \frac{p}{p_*}, \quad p_* = \frac{\mu D_{K,h}}{B_0} \qquad [9]$$

and setting $Q = 3$, Eqs. 6, 7 transform to

$$\frac{\partial(y\tilde{p})}{\partial\tilde{x}} + y\tilde{p}\frac{\partial\tilde{p}}{\partial\tilde{x}} = -(1+K)\tilde{N}_h \qquad [10]$$

$$(1 + \tilde{p}\,(3-2y))\frac{\partial\tilde{p}}{\partial\tilde{x}} = 2\tilde{N}_h \qquad [11]$$

where the dimensionless hydrogen molar flux is

$$\tilde{N}_h = \frac{N_h}{N_*}, \quad N_* = \frac{\mu D_{K,h}^2}{RTLB_0} \qquad [12]$$

Mass transport equations.—Hydrogen mass conservation in the ASL prescribes that

$$\frac{\partial\tilde{N}_h}{\partial\tilde{x}} = 0. \qquad [13]$$

Differentiating Eqs. 10, 11 over $\tilde{x}$, we thus get

$$\frac{\partial}{\partial\tilde{x}}\left(\frac{\partial(y\tilde{p})}{\partial\tilde{x}} + y\tilde{p}\frac{\partial\tilde{p}}{\partial\tilde{x}}\right) = 0 \qquad [14]$$

$$\frac{\partial}{\partial\tilde{x}}\left((1 + \tilde{p}\,(3-2y))\frac{\partial\tilde{p}}{\partial\tilde{x}}\right) = 0 \qquad [15]$$

It is worth noting that the system of Eqs. 14, 15 does not contain parameters. Eqs. 14, 15 form a system of two second–order nonlinear elliptic Eqs. for y and $\tilde{p}$. Eqs. 10, 11 are the first integral of Eqs. 14, 15 and below, Eqs. 10, 11 will be analyzed further.

Boundary (initial) conditions.—At the channel/ASL interface $y = y_c$, $\tilde{p} = \tilde{p}_c$. where the subscript c marks the values in the channel. The reaction stoichiometry prescribes that the hydrogen flux $N_h = J/(2F)$, or $\tilde{N} = \tilde{J}$ (see below). Setting in Eq. 10 $\tilde{x} = 0$ and expanding the derivative in the first term, we get

$$\tilde{p}_c\frac{\partial y}{\partial\tilde{x}}\bigg|_{\tilde{x}=0} = -y_c(1+\tilde{p}_c)\frac{\partial\tilde{p}}{\partial\tilde{x}}\bigg|_{\tilde{x}=0} - (1+K)\tilde{J} \qquad [16]$$

where

$$\tilde{J} = \frac{J}{J_*}, \quad J_* = 2FN_* = \frac{2F\mu D_{K,h}^2}{RTLB_0} \qquad [17]$$

Quite similarly, setting $\tilde{x} = 0$ in Eq. 11, we find

$$\left.\frac{\partial \tilde{p}}{\partial \tilde{x}}\right|_{\tilde{x}=0} = \frac{2\tilde{J}}{1 + \tilde{p}_c(3 - 2y_c)} \equiv W \qquad [18]$$

Conservation Law and Approximate Analytical Solution

Since $\tilde{N}_h = \tilde{J}$, Eqs. 10, 11 can be written as

$$\frac{\partial(y\tilde{p})}{\partial \tilde{x}} + y\tilde{p}\frac{\partial \tilde{p}}{\partial \tilde{x}} = -(1 + K)\tilde{J} \qquad [19]$$

$$\left(1 + \tilde{p}\,(3 - 2y)\right)\frac{\partial \tilde{p}}{\partial \tilde{x}} = 2\tilde{J} \qquad [20]$$

With the constant right sides, Eqs. 19, 20 automatically satisfy the mass transport Eqs. 14, 15. Multiplying Eq. 19 by 2 and summing with Eq. 20, we get

$$2\frac{\partial(y\tilde{p})}{\partial \tilde{x}} + (1 + 3\tilde{p})\frac{\partial \tilde{p}}{\partial \tilde{x}} = -2K\tilde{J} \qquad [21]$$

Rewriting this equation as

$$2\frac{\partial(y\tilde{p})}{\partial \tilde{x}} + \frac{\partial \tilde{p}}{\partial \tilde{x}} + \frac{3}{2}\frac{\partial(\tilde{p}^2)}{\partial \tilde{x}} = -2K\tilde{J} \qquad [22]$$

we see that it can be integrated from 0 to $\tilde{x}$ yielding a conservation law:

$$2(y\tilde{p} - y_c\tilde{p}_c) + (\tilde{p} - \tilde{p}_c) + \frac{3}{2}(\tilde{p}^2 - \tilde{p}_c^2) = -2K\tilde{J}\,\tilde{x} \qquad [23]$$

An analogue of Eq. 23 can be derived for the two–component CO-CO_2 system. Equation 19 does not change, while Eq. 7 in the dimensionless form reads

$$(1 + \tilde{p}\,(Q - y(Q - 1)))\frac{\partial \tilde{p}}{\partial \tilde{x}} = -(1 - Q)\tilde{J} \qquad [24]$$

Multiplying Eq. 19 by $(Q - 1)$ and summing with Eq. 24 we get

$$(Q - 1)\frac{\partial(y\tilde{p})}{\partial \tilde{x}} + (1 + Q\tilde{p})\frac{\partial \tilde{p}}{\partial \tilde{x}} = -(Q - 1)K\tilde{J} \qquad [25]$$

Integrating Eq. 25 from 0 to $\tilde{x}$ we find

$$(Q - 1)(y\tilde{p} - y_c\tilde{p}_c) + (\tilde{p} - \tilde{p}_c) + \frac{Q}{2}(\tilde{p}^2 - \tilde{p}_c^2) = -(Q - 1)K\tilde{J}\,\tilde{x} \qquad [26]$$

where $Q = \sqrt{44/28}$ for the CO-CO_2 pair.

A simple analytical formula for the hydrogen molar fraction through the ASL depth can be obtained from the conservation law as follows. The pressure $\tilde{p}$ slightly increases along $\tilde{x}$, while the hydrogen molar fraction y decreases. The variation of the product $\tilde{p}y$ along $\tilde{x}$ is not large and hence the factor $\left(1 + \tilde{p}\,(3 - 2y)\right)$ in Eq. 20 does not change much along $\tilde{x}$. Thus, the deviation of $\partial\tilde{p}/\partial\tilde{x}$ in Eq. 20 from a constant value is expected to be small. From Eq. 18 it follows that a reasonably good approximation for $\tilde{p}(\tilde{x})$ is a linear function

$$\tilde{p} \simeq \tilde{p}_c + W\tilde{x} \qquad [27]$$

Solving Eq. 23 for y and substituting $\tilde{p}$, Eq. 27, into the resulting equation, we get

$$y = \frac{1}{\tilde{p}_c + W\tilde{x}}\left(y_c\tilde{p}_c - \frac{3}{4}W^2\tilde{x}^2 - \left(\frac{(3\tilde{p}_c + 1)}{2}W + K\tilde{J}\right)\tilde{x}\right) \qquad [28]$$

At $\tilde{x} = 1$, multiplying Eqs. 28 and 27 we get the hydrogen molar concentration $c_a = p_*\tilde{p}_a y_a/(RT)$ at the active layer:

$$c_a = \frac{p_*}{RT}\left(y_c\tilde{p}_c - \frac{3}{4}W^2 - \left(\frac{(3\tilde{p}_c + 1)}{2}W + K\tilde{J}\right)\right), \quad \text{mol m}^{-3} \qquad [29]$$

Similar results for CO-CO_2 mixture can be easily derived from Eqs. 26, 27. Cell performance models include calculation of the anode concentration polarization, which requires an accurate value of the hydrogen concentration c_a in the anode active layer. Equation 29 gives a more accurate value of this parameter. The anode transport overpotential η_{tra} can be estimated using the Nernst equation

$$\eta_{tra} = \frac{RT}{2F}\ln\left(\frac{c_c c_{w,a}}{c_a c_{w,c}}\right) = \frac{RT}{2F}\ln\left(\frac{c_c(c_{t,a} - c_a)}{c_a(c_{t,c} - c_c)}\right) \qquad [30]$$

where the subscripts c, a denote the channel and the active layer, and the subscript t denotes the total molar concentration. In this equation, c_a is given by Eq. 29, $c_{t,a} = p_a/(RT)$, where p_a is given by Eq. 27 with $\tilde{x} = 1$ and the other parameters are those in the channel. Note that Eq. 30 gives a rough estimate for η_{tra}, since the Nernst equation is not strictly valid in non–equilibrium conditions.

Results and Discussion

The parameters used in the calculations below are collected in Table I. The transport coefficients have been calculated as

$$B_0 = \frac{\lambda d^2}{32}, \quad \text{Ref. [14]}$$
$$D_{K,h} = \frac{\lambda d}{3}\sqrt{\frac{8RT}{\pi M_h}}$$
$$D_m = \lambda D_m^{free} \qquad [31]$$

where λ is the porosity/tortuosity ratio, d is the mean pore diameter (Table I). The numerical solution to Eqs. 19, 20 was obtained using the standard Python BVP solver *solve_bvp*.

Setting in Eq. 23 $\tilde{p} = \tilde{p}_c$ we obtain the linear hydrogen molar fraction shape (Fick's law) corresponding to zero pressure gradient in the ASL:

$$y = y_c - \frac{RTLJ}{2FD_m p_c}\frac{x}{L} \qquad [32]$$

In the literature, another version of the Fick's law, which follows from the SMKM has been used:[15,16]

Table I. Cell parameters used in calculations.

Cell temperature, K	T	273 + 800
Pressure in the channel, Pa	p_c	10^5
Current density, A m^{-2}	J	10^4
Anode thickness, m	L	10^{-3}
Mean pore diameter, m	d	10^{-6}
Porosity/tortuosity ratio	λ	0.033, Ref. 6
Hydrogen viscosity at 800 °C, Pa s	μ	$2 \cdot 10^{-5}$
Free binary molecular diff. m^2 s^{-1}	D_m^{free}	$8.154 \cdot 10^{-4}$, Ref. 6
Anode gas composition		85%H_2 + 15%H_2O

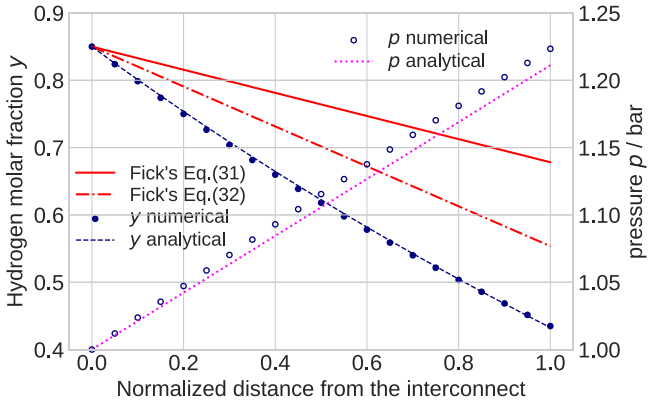

Figure 2. The shapes of hydrogen molar fraction through the one–mm thick Ni–YSZ cermet anode calculated using the Fick's law Eq. 32 (solid line), Eq. 33 (dash-dotted line), from the numerical solution to the DGM model Eqs. 19, 20 (solid points), and using the analytical solution Eq. 28 (dashed line). Open circles show numerical pressure from the DGM model (right axis), dotted line is the approximate linear formula for $p(\tilde{x})$, Eq. 27.

$$y = y_c - \frac{RTLJ}{2Fp_c}\left(\frac{1}{D_m} + \frac{1}{D_{K,h}}\right)\frac{x}{L} \qquad [33]$$

Figure 2 shows the linear shapes of y from the Fick's law, Eqs. 32 and 33, the exact numerical solution to the problem 19, 20, and the approximate analytical Eq. 28. The numerical and analytical, Eq. 27, shapes of pressure are also shown.

Both Fick's equations, Eqs. 32, 33 quite significantly overestimate the exact hydrogen molar fraction (Fig. 2). Physically, Knudsen diffusion leads to formation of the positive pressure gradient (Fig. 2), which retards hydrogen diffusion toward the active (reaction) zone, while the Fick's equations ignore this effect. Furthermore, the Fick's law is used in literature together with the constant pressure assumption, so the error in the calculated hydrogen molar concentration $c = yp/(RT)$ is even larger than the error in y itself shown in Fig. 2.

The analytical shape of hydrogen molar fraction, Eq. 28, approximates the numerical result very well (Fig. 2). The linear shape of pressure, Eq. 27, is somewhat less accurate, though the maximal error at the ASL/active layer interface is about 1% only (Fig. 2). It is worth noting that for lower currents, the agreement of analytical and numerical pressure shapes is better. Eq. 29 could, thus, be recommended for calculation of concentration polarization in SOFC anode instead of a widely used Fick's law.

The Fick's law, Eq. 32 results from the conservation law under the condition $\partial\tilde{p}/\partial\tilde{x} = 0$ and it shows that y is independent of the Knudsen diffusivity. Therefore, in the case of H_2-H_2O mixture, the Stefan–Maxwell–Knudsen model, Eq. 4, and in particular Eq. 33, is contradictory. Indeed, from Eq. 32 it follows that to neglect the pressure gradient in Eq. 3, *both* $\partial p/\partial x$ and Knudsen $N_k/D_{K,k}$ terms must be omitted, rather than just the term $\partial p/\partial x$.

From Eq. 27 an accurate condition for neglecting the pressure gradient term can be derived. The pressure variation through the ASL is small if the second term in Eq. 27 at $\tilde{x} = 1$ is much less than $\tilde{p}_c$. Thus, the required condition is $W/\tilde{p}_c \ll 1$ and from Eq. 18 we find

$$\frac{2\tilde{J}}{(1 + \tilde{p}_c(3 - 2y_c))\tilde{p}_c} \ll 1 \qquad [34]$$

In dimensional form Eq. 34 reads

$$\frac{JRTL}{FD_{K,h}\left(1 + \frac{p_c B_0(3-2y_c)}{\mu D_{K,h}}\right)p_c} \ll 1 \qquad [35]$$

The hydraulic permeability B_0 is quadratic in the pore diameter d, while the hydrogen Knudsen diffusivity $D_{K,h}$ is linear in d, Eqs. 31. Thus, for sufficiently small d, the second term in the denominator of Eq. 35 can be neglected and this equation simplifies to

$$\frac{JRTL}{FD_{K,h}p_c} \ll 1 \qquad [36]$$

Equation 36 does not contain B_0, i.e., the only process responsible for the pressure gradient buildup is the Knudsen diffusion. For small d, $D_{K,h}$ is also small and Eq. 36 is satisfied if the current density J is sufficiently small.

In the opposite limit of large pore diameter, the unit in the denominator of Eq. 35 can be neglected and this equation simplifies to

$$\frac{JRTL\mu}{FB_0(3 - 2y_c)p_c^2} \ll 1 \qquad [37]$$

As expected, Eq. 37 is independent of the Knudsen diffusivity, i.e. the pressure gradient is developed by the finite hydraulic permeability of the anode. At high cell current and/or low pressure in the anode channel Eq. 37 may be violated.

The general condition for the smallness of the pressure gradient is given by Eq. 35. With the data in Table I, the left side of Eq. 35 is 0.21 (Fig. 2), showing that the pressure gradient term is quite significant. However, for the four times larger mean pore diameter, the left side of Eq. 35 decreases to 0.036, indicating that the pressure variation through the ASL is small. In this case, the solutions derived above are of course valid, though the simpler Eq. 33 is equally accurate.

Fu et al.[4] reported detailed numerical analysis of the DGM solutions for the SOFC anode. They showed that in the electrode with sufficiently large pore diameter, the pressure gradient term can be neglected and the isobaric DGM, which is equivalent to the SMKM above can be used. In their experiments, the anode thickness was 1.5 mm, the estimated anode porosity/tortuosity ratio was 0.1 (Fig. 11[4]) and the mean pore diameter was around 2 μm. The anode hydraulic permeability B_0 was not specified in Ref. 4 and for the estimate we use Eq. 31. The remaining parameters, including the cell current density are taken from Table I. With this set of parameters the left side of Eq. 35 is 0.048, i.e., the pressure at the active layer exceeds the pressure in the channel by 5% only. Under these conditions, in the case of H_2–H_2O mixture the isobaric approximation works quite well, as reported in Ref. 4. Note that Fu et al.[4] considered also a triple gas mixture H_2–H_2O–N_2 and due to the presence of N_2 Eq. 35 may underestimate the pressure gradient. Calculations of Fu et al. show that the nitrogen molar fraction decreases toward the active layer, i.e. the diffusion flux of nitrogen is directed toward the active layer. Thus, to keep the total nitrogen flux at zero, a higher $\partial p/\partial x$ is required to support a counterflow of nitrogen toward the anode channel.

Generally, if the anode transport parameters are available, estimation with Eq. 35 allows to select the appropriate approximation for the hydrogen molar fraction in the electrode. However, it is more safe to use the Eqs. from the previous section, which are valid for any set of anode transport and operating parameters.

The conservation law, Eq. 23, provides several opportunities. Setting in Eq. 23 $\tilde{x} = 1$, we get a relation between parameters in the channel and at the ASL/active layer interface:

$$2(y_a\tilde{p}_a - y_c\tilde{p}_c) + (\tilde{p}_a - \tilde{p}_c) + \frac{3}{2}(\tilde{p}_a^2 - \tilde{p}_c^2) = -2K\tilde{J} \qquad [38]$$

where the subscript a marks the values at $\tilde{x} = 1$. In dimensional form Eq. 38 reads

$$2(y_a p_a - y_c p_c) + p_a - p_c + \frac{3}{2}(p_a^2 - p_c^2)\frac{B_0}{\mu D_{K,h}} = -\frac{RTLJ}{FD_m} \qquad [39]$$

From a practical perspective, by measuring the pressure p_a one can calculate the hydrogen molar fraction y_a in the active layer using Eq. 39. Other useful options arise in the case of limiting current density: setting in Eq. 39 $y_a = 0$, we get the relation between y_c, p_c, p_a and the system transport parameters:

$$-2y_c p_c + p_a - p_c + \frac{3}{2}(p_a^2 - p_c^2)\frac{B_0}{\mu D_{K,h}} = -\frac{RTLJ}{FD_m} \qquad [40]$$

Eq. 40 allows direct calculation of the pressure p_a at the active layer. On the other hand, by measuring p_a in this regime the relationship between $D_{K,h}$, B_0 and D_m is obtained, so any one of these three transport parameters can be estimated if the other two are known. Measuring the pressure inside of the porous sandwich at high temperature is a challenging task.[17] However, it may be feasible in the future.

Finally, we note that the analytical shapes Eqs. 27, 28 can be used to develop a fast analytical model for the anode impedance. This work is in progress and the results will be published elsewhere. Note also that the hydrogen transport in the Solid Oxide Electrolysis Cells (SOECs) could be described by the same model.

Conclusions

An exact first integral (the conservation law) of the Dusty–Gas Model for the two-component mixture transport in the SOFC anode support layer is derived. Based on this result, an approximate analytical solutions for the hydrogen molar fraction and total pressure shapes in the ASL are obtained. Comparison with the numerical solution of the full system of DGM Eqs. shows the good quality of the approximate solutions. A simple formula for the hydrogen molar fraction at the ASL/active layer interface could be used instead of the Fick's law for a more accurate calculation of the concentration overpotential. A condition for neglecting the pressure gradient effects is derived and several possibilities for measuring the electrode transport parameters provided by the conservation law are discussed.

ORCID

Andrei Kulikovsky https://orcid.org/0000-0003-1319-576X

References

1. E. A. Mason and A. P. Malinauskas, *Transport in Porous Media: The Dusty Gas Model* (Elsevier) (1983).
2. A. McEvoy, "Anodes." *High Temperature Solid Oxide Fuel Cells. Fundamentals, Design and Applications*, ed. S. C. Singhal and K. Kendall (Elsevier)149 (2003).
3. H. Zhu and R. J. Kee, "Modeling distributed charge–transfer processes in SOFC membrane–electrode assemblies." *J. Electrochem. Soc.*, **155**, B715 (2008).
4. Y. Fu, Y. Jiang, S. Poizeau, A. Dutta, A. Mohanram, J. D. Pietras, and M. Z. Bazant, "Multicomponent gas diffusion in porous electrodes." *J. Electrochem. Soc.*, **162**, F613 (2015).
5. W. Lehnert, J. Meusinger, and R. Thom, "Modeling of gas transport phenomena in SOFC anodes." *J. Power Sources*, **87**, 57 (2000).
6. C. Bao and N. Cai, "An approximate analytical solution of transport model in electrodes for anode–supported solid oxide fuel cells." *AIChE J.*, **53**, 2968 (2007).
7. Y. Shi, N. Cai, C. Li, C. Bao, E. Croiset, J. Qian, Q. Hu, and S. Wang, "Simulation of electrochemical impedance spectra of solid oxide fuel cells using transient physical models." *J. Electrochem. Soc.*, **155**, B270 (2008).
8. F. N. Cayan, S. R. Pakalapati, F. Elizalde-Blancas, and I. Celik, "On modeling multi-component diffusion inside the porous anode of solid oxide fuel cells using Fick's model." *J. Power Sources*, **192**, 467 (2009).
9. A. Hffelin, J. Joos, M. Ender, A. Weber, and E. Ivers-Tiffe, "Time-dependent 3D impedance model of mixed-conducting solid oxide fuel cell cathodes." *J. Electrochem. Soc.*, **160**, F867 (2013).
10. F. Yang, J. Gu, L. Ye, Z. Zhang, G. Rao, Y. Liang, K. Wen, J. Zhao, J. B. Goodenough, and W. He, "Justifying the significance of Knudsen diffusion in solid oxide fuel cells." *Energy*, **95**, 242 (2016).
11. R. Krishna and J. A. Wesselingh, "The Maxwell–Stefan approach to mass transfer." *Chem. Eng. Sci.*, **52**, 861 (1997).
12. H. Zhu, R. J. Kee, V. M. Janardhanan, O. Deutschmann, and D. Goodwin, "Modeling electrochemical impedance spectra in SOFC button cells with internal methane reforming." *J. Electrochem. Soc.*, **152**, A2427 (2005).
13. I. K. Kookos, "On the diffusion in porous electrodes of SOFCs." *Chem. Engineer. Sci.*, **69**, 571 (2012).
14. A. Bertei and C. Nicolella, "Common inconsistencies in modeling gas transport in porous electrodes: The dusty-gas model and the Fick law." *J. Power Sources*, **279**, 133 (2015).
15. R. Suwanwarangkul, E. Croiset, M. W. Fowler, P. L. Douglas, E. Entchev, and M. A. Douglas, "Performance comparison of Fick's, dusty–gas and Stefan–Maxwell models to predict the concentration overpotential of a SOFC anode." *J. Power Sources*, **122**, 9 (2003).
16. J. Ma, M. Yan, Y. Zhang, and S. Quin, "Analysis of mass transport in solid oxide fuel cells using a thermodynamically consistent model." *Int. J. Energy Res.*, **46**, 6487 (2022).
17. M. Nagata and H. Iwahara, "The measurement of water vapour pressure in an SOFC anode during discharge." *J. Appl. Electrochem.*, **23**, 275 (1993).